Earthquake Engineering & Structural Dynamics
The Journal of the International Association for Earthquake Engineering

EARTHQUAKE ENGINEERING & STRUCTURAL DYNAMICS
Earthquake Engng Struct. Dyn. 2013; **42**:1375–1394
Published online 25 January 2013 in Wiley Online Library (wileyonlinelibrary.com). DOI: 10.1002/eqe.2277

Seismic performance of highway bridges with fusing bearing components for quasi-isolation

Evgueni T. Filipov[1], Jessica R. Revell[1], Larry A. Fahnestock[1,*,†], James M. LaFave[1], Jerome F. Hajjar[2], Douglas A. Foutch[1] and Joshua S. Steelman[1]

[1]*Department of Civil and Environmental Engineering, University of Illinois at Urbana-Champaign, 205 North Mathews Avenue, Urbana, IL 61801, U.S.A.*
[2]*Department of Civil and Environmental Engineering, Northeastern University, 400 Snell Engineering Center, 360 Huntington Avenue, Boston, MA 02115, U.S.A.*

SUMMARY

Modern highway bridges in Illinois are often installed with economical elastomeric bearings that allow for thermal movement of the superstructure, and steel fixed bearings and transverse retainers that prevent excessive movement from service-level loadings. In the event of an earthquake, the bearing system has the potential to provide a quasi-isolated response where failure of sacrificial elements and sliding of the bearings can cause a period elongation and reduce or cap the force demands on the substructure. A computational model that has been calibrated for the expected nonlinear behaviors is used to carry out a parametric study to evaluate quasi-isolated bridge behavior. The study investigates different superstructure types, substructure types, substructure heights, foundation types, and elastomeric bearing types. Overall, only a few bridge variants were noted to unseat for design-level seismic input in the New Madrid Seismic Zone, indicating that most structures in Illinois would not experience severe damage during their typical design life. However, Type II bearing systems, which consist of an elastomeric bearing and a flat PTFE slider, would in some cases result in critical damage from unseating at moderate and high seismic input. The sequence of damage for many bridge cases indicates yielding of piers at low-level seismic input. This is caused by the high strength of the fixed bearing element, which justifies further calibration of the quasi-isolation design approach. Finally, the type of ground motion, pier height, and bearing type were noted to have significant influence on the global bridge response. Copyright © 2013 John Wiley & Sons, Ltd.

Received 1 February 2012; Revised 2 December 2012; Accepted 3 December 2012

KEY WORDS: seismic isolation; quasi-isolation; highway bridges; sliding bearings; earthquake response history analysis

1. INTRODUCTION

Seismic isolation is a well-accepted design philosophy for bridges in high seismic regions of the USA [1, 2]. Although seismic isolation can provide a high level of structural performance, the design complexity and higher cost of construction make this approach less attractive in regions of the country such as Illinois where a potential for large earthquakes exists, but only at long recurrence intervals. As a result, the concept of quasi-isolation for bridges has emerged as an innovative, yet pragmatic, design philosophy that can be broadly applied. The basic notion of quasi-isolation is that typical bridge bearing systems can be designed and detailed such that they act as fuses to limit the forces transmitted from the superstructure to the substructure, while accommodating the concomitant

*Correspondence to: Larry A. Fahnestock, Department of Civil and Environmental Engineering, University of Illinois at Urbana-Champaign, 2108 Newmark Civil Engineering Laboratory, 205 North Mathews Avenue, Urbana, IL 61801, U.S.A.
†E-mail: fhnstck@illinois.edu

displacements. A prime difference between classical isolation [3] and the system studied in this paper is that quasi-isolation does not require a complex design process, yet can provide damage mitigation for significant seismic events. This philosophy, which was initially developed by the Illinois Department of Transportation (IDOT), is intended to provide a cost-effective bridge with an earthquake-resisting system (ERS) [2] that limits damage for small seismic events and still prevents span loss during a strong event in the New Madrid Seismic Zone (NMSZ). At the core of the IDOT ERS is an extension of a common bridge design methodology employed in higher seismic regions of the USA, where the substructure and superstructure should remain elastic while a specific fusing mechanism is implemented at the interface between the two [4, 5]. The concept of the IDOT ERS allows for the following three distinct levels of fusing and redundancy: Level 1—permitting damage and failure of the bearing components to allow quasi-isolation, Level 2—providing sufficient seat widths to permit the required sliding, and Level 3—permitting some damage to the substructure so long as there is no span loss.

The research described in this paper is part of a broad program to calibrate and refine the IDOT ERS for common highway bridges with simply supported abutment conditions and continuous spans. The overall research program, discussed in detail in previous publications [6], has six primary components: (i) conducting full-scale tests of typical bridge bearings used in Illinois; (ii) developing numerical models of bridge bearings, validated against test results; (iii) exploring local response of bearings not considered experimentally; (iv) developing numerical models of full bridge systems, which capture all important aspects of behavior; (v) conducting parametric studies to explore system level seismic response for a range of representative Illinois bridges; and (vi) developing recommendations for seismic design of bridges using the quasi-isolation philosophy. This paper focuses on the fifth component of the research program, by providing quantitative and qualitative evaluation of the quasi-isolation system's seismic response.

Many existing bridges in Illinois have the potential to achieve a response that would be considered as quasi-isolation. For thermal expansion, these bridges use steel-reinforced elastomeric bearings, which are either (1) IDOT Type I bearings that are placed directly on the concrete substructure (vulcanized to only a top steel plate) or (2) IDOT Type II bearings, which consist of the following: a bottom steel plate bolted to the substructure and vulcanized to the elastomeric component, a middle plate that is vulcanized to the top of the elastomer and coated on top with polytetrafluoroethylene (also known as PTFE or Teflon), and a top plate with a stainless steel mating surface carrying the girder load directly onto the PTFE surface. Transverse serviceability movements at the elastomeric bearings are limited by stiffened angle side retainers. Low-profile fixed steel bearings are placed at one intermediate substructure with the intent to carry traffic braking loads and prevent global service load movement of the structure. Preliminary design procedures in the IDOT Bridge Manual [7] aim to proportion retainers and fixed bearings to have lateral capacities equal to 20% of the dead load at the bearing of interest, with the intent that these steel components will exhibit nonlinear behaviors and fail at high seismic loads. The IDOT bridge design procedures are intended primarily for typical bridges in seismic Zones 1, 2 and 3 as defined by the American Association of State Highway and Transportation Officials (AASHTO). Bridges with complex geometries and in locations of high seismic hazard (Zone 4) are encouraged to utilize more advanced analysis and design techniques than prescribed in the IDOT Bridge Manual.

Recent work by Filipov *et al*. [8] developed nonlinear bearing and retainer element models that are based on early experimental results from this project and are capable of simulating unique aspects of the cyclic bearing component response (e.g., elastomer shear deformations, friction (stick–slip), and nonlinear retainer failure). The nonlinear elements were implemented into a global prototype bridge model used for static pushover analyses of the quasi-isolated system. That same prototype model is the basis for the analyses described in this paper.

Section 2 of this paper briefly describes the prototype model, outlines the variations in the parametric space considered in this study, and discusses calibration of the bearing models. In Section 3, the input ground motion considerations are discussed, to give a basis for the incremental dynamic analyses (IDAs) carried out for each of the bridges. Section 4 discusses damage limit states that can be encountered in an earthquake and shows a sample dynamic analysis of a single bridge structure. Section 5 provides an overall evaluation of the seismic performance for typical bridge systems in Illinois.

DOI: 10.1002/eqe

2. OVERVIEW OF NONLINEAR MODELING FOR PARAMETRIC VARIATIONS

2.1. Basic bridge prototype

The base prototype bridge in Figure 1, is a three-span continuous steel I-girder superstructure on multi-column (4) pier substructures (all proportioned in accordance with the IDOT Bridge Manual [7]). The bridge deck allows for two lanes of traffic, and it is constructed with six W27x84 (AASHTO M270 Gr. 50) steel girders that act compositely with a 20.3 cm (8 in.)-thick concrete deck. All deck elements (including the diaphragm elements) are modeled as linear with appropriate elastic stiffness.

The multi-column piers are 4.5 m (15 ft) tall and are modeled with beam–column elements with hinges and fiber sections that capture material nonlinearities in the concrete and reinforcement. The prototype system is modeled with a fixed base, representing a stiff, steadfast foundation on a rocky substrate. The nonlinear behavior of the abutment backwalls is modeled with a 5 cm (2 in.) gap simulating a thermal expansion cavity, and a hyperbolic material model is used to capture the backfill behavior. For the typical three-span bridge configuration used in this parametric study, low-profile fixed bearings are installed at the second pier (Pier 2), while Type I or Type II elastomeric expansion bearings are used at the other pier and at the abutments. The base prototype bridge uses Type I elastomeric bearings where sliding occurs at the elastomer-concrete interface. Stiffness and mass proportional damping of 5% is used in the first longitudinal and transverse modes, and additional damping occurs from hysteretic behavior of the nonlinear elements. Detailed information on the global bridge model and the component formulations is contained in previous publications [6, 8].

2.2. Parametric variations

The parametric variations studied in this paper were based on the current bridge stock in Illinois as defined in [9], as well as current trends of bridge design in Illinois, where elastomeric bearings are now the preferred type of expansion bearing. At the time of the previous study, 75% of the bridges had three spans with total lengths ranging from 33 to 82 m (110–270 ft), and consisted of 86% steel girders and 14% concrete girders with composite decks; 67% had multi-column piers, 32% had wall piers, and heights ranged from 2.7 m (9 ft) to 14 m (46 ft). Site conditions ranged from Class B to E soils, foundations consisted primarily of piles (86%), and 33% of bridges had elastomeric bearings [9].

The bridges investigated herein incorporate variations in superstructure type, substructure type, substructure height, foundation type, and elastomeric bearing system, and provide a reasonable representation of modern bridges in Illinois. On the other hand, bridges with simply supported spans, steel rocker bearings, integral abutments, or curved superstructures are not considered in this study. Bridge model variations are named with a series of letters and numbers to provide a nomenclature for the parameters used in the study. The first two letters of the model name indicate the superstructure type, (Ss, steel short; Sl, steel long; Cs, concrete short). The third letter and the following two numbers designate the intermediate substructure type (C, column pier; W, wall pier) and height in feet (15 ft (4.5 m) and 40 ft (12.2 m)). The next letter and number indicate the bearing type used (T1, Type I IDOT bearing; T2, Type II IDOT bearing). The final letter indicates the foundation boundary condition flexibility (F, fixed/rock; S, flexible foundation boundary condition). The flexible boundary condition simulates a group pile foundation with a pile cap in soft soils. It should be noted that foundation boundary condition is an independent variable from the ground motion properties that are defined in Section 3.

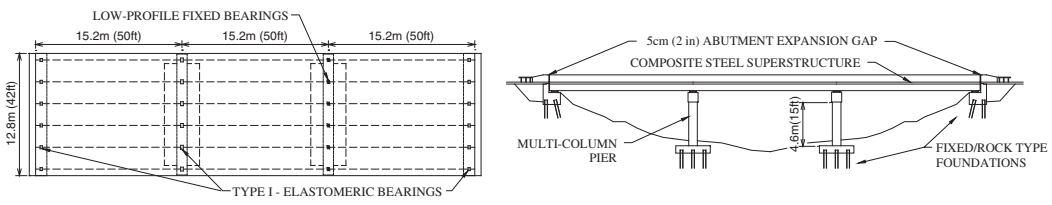

(a) Plan (b) Elevation

Figure 1. Base bridge prototype.

DOI: 10.1002/eqe

With the provided definitions, the base prototype bridge can be denoted as SsC15T1F, whereas SlW40T2S would indicate a bridge with a long steel superstructure, supported on 12.2 m (40 ft) wall piers with flexible foundation boundary conditions and Type II IDOT bearings. Later in this paper, the symbols 'X', 'x', and '#' are used to designate all the variations of a particular parameter. Bridge variations defined using this nomenclature result in 48 distinct bridges that are studied in this research. Details on the various parameters used are shown in Table I, and two sample meshes of the finite element bridge models created with OpenSees [10] are shown in Figure 2.

2.3. Calibration of the bi-directional sliding bearing elements

Bearing systems modeled with uncoupled, uniaxial elements are considered unreliable for multi-directional seismic analysis. For example, friction pendulum isolators modeled with uncoupled elements resulted in overestimation of forces and underestimation of system displacements, when compared with bi-directional coupled models and experimental data [11, 12]. Although friction pendulum bearings are not considered herein, the findings related to modeling are applicable to other types of isolation systems, and therefore, an orthogonally coupled, zero-length, bi-directional model (similar to that presented in [13]) was created for the modeling of friction stick–slip behaviors exhibited by Type I and Type II IDOT bearings. The model, shown schematically in Figure 3(b), is capable of capturing an initial static friction break-off force (P_{SI}), a kinetic friction force (P_K), and a post-slip friction break-off force (P_{SP}). Different coefficients of friction are specified for each condition, and the variable axial load on the bearing is used in the model formulation.

Experimental results from this project [14, 15] were used to inform the behavior of the sliding bearings, and sample model validation is shown in Figure 3. The Type I bearings were modeled with a static initial coefficient of friction of $\mu_{SI} = 0.60$, a kinetic coefficient of friction of $\mu_K = 0.45$, and a post-slip coefficient of static friction of $\mu_{SP} = 0.50$. The Type II bearings were simulated with $\mu_{SI} = 0.16$ and $\mu_{SP} = \mu_K = 0.15$. The stiffness of the elastomeric bearings is calculated as the effective apparent shear modulus of the elastomer, approximated as 585 kPa (85 psi) on the basis of experimental data for strain levels sufficient to induce slip on concrete, times the plan area of the bearing divided by the total height of rubber (h_{rt}). Monotonic and cyclic tests of the Type I bearings showed reliable and resilient behavior for large vertical bearing forces and large magnitudes of bearing travel. Type II bearings also showed reliable sliding behavior; however, at large top plate displacements, these bearings exhibit unstable behavior that requires increasingly larger forces to re-center the bearing. This instability is believed to rapidly move the bearing into an unseated configuration, where the model as shown in Figure 3(b) will become invalid. This response is discouraged for quasi-isolation and is discussed in further detail in Section 4.1.

2.4. Calibration of the uni-directional retainer elements

The retainers placed in the transverse direction of each elastomeric bearing were shown to exhibit roughly elasto-plastic behavior on the basis of experimental testing [14]. The failure mode consisted of localized concrete crushing (primarily for larger anchor bolts) and subsequent bolt tensile–shear failure. A nonlinear uni-axial model has been formulated [8] that utilizes an initial gap followed by elasto-plastic response and a subsequent failure criterion at an ultimate displacement. Current design specifications state that retainers should be installed at a gap of 3.2 mm (0.125 in.); however, the experiments showed that an additional gap of 7.6 mm (0.3 in.) should be assumed in analysis because the oversized bolt hole in the retainer leaves additional space between the anchor bolt and the edge of the retainer hole, and force is not developed upon instantaneous contact of the retainers. A variation of the IDOT design equation [7] for strength of retainers was found to be satisfactory for predicting the ultimate force capacity of the retainer element, with

$$P_{RET\_EXPECTED} = \varphi 0.8 A_b F_u \tag{1}$$

where A_b is the nominal anchor bolt area, F_u is the ultimate tensile strength, and $\varphi = 1$ for no strength reduction. The model elastic and plastic stiffnesses were set to $E_E = 790$ MPa (115 ksi) and $E_P = 57$ MPa (8 ksi), respectively, and the ratio of ultimate to yield strength $P_{RET\_EXPECTED}/P_{RET\_Y} = 1.80$, were based

DOI: 10.1002/eqe

Table I. Specifications for various bridge parameters.

Superstructure information	Steel short (Ss)		Steel long (Sl)		Concrete short (Cs)	
Girder size	W27x84 US		W40x183 US		91.4 cm (36 in.) PPC I-Girder	
Span lengths	15.2–15.2–15.2 m (50–50–50 ft)		24.4–36.6–24.4 m (80–120–80 ft)		18.3–18.3–18.3 m (60–60–60 ft)	
Superstructure weight	92 kN/m (6.28 kip/ft)		100 kN/m (6.85 kip/ft)		119 kN/m (8.17 kip/ft)	
Abutment bearing information						
Type I	9-b		15-e		9-c	
Plan dims.	23 × 30 cm (9 × 12 in.)		38 × 61 cm (15 × 24 in.)		23 × 30 cm (9 × 12 in.)	
Total height of rubber (hrt)	6.7 cm (2.6 in.)		13.3 cm (5.25 in.)		7.6 cm (3 in.)	
Type II	7-b		9-b		9-a	
Plan dims.	18 × 30 cm (7 × 12 in.)		23 × 30 cm (9 × 12 in.)		23 × 30 cm (9 × 12 in.)	
Total height of rubber (hrt)	3.8 cm (1.5 in.)		6.7 cm (2.6 in.)		4.8 cm (1.9 in.)	
Ret. anchor bolt dia.	1.6 cm (0.625 in.)		1.9 cm (0.75 in.)		1.9 cm (0.75 in.)	
$P_{RET\_EXPECTED}$	65 kN (15 kips)		94 kN (21 kips)		94 kN (21 kips)	
Pier bearing information						
Type I	11-a		15-b		13-a	
Plan dims.	28 × 41 cm (11 × 16 in.)		38 × 61 cm (15 × 24 in.)		33 × 51 cm (13 × 20 in.)	
Total height of rubber (hrt)	6.7 cm (2.6 in.)		13.3 cm (5.25 in.)		7.6 cm (3 in.)	
Type II	11-a		15-b		13-a	
Plan dims.	28 × 41 cm (11 × 16 in.)		38 × 61 cm (15 × 24 in.)		33 × 51 cm (13 × 20 in.)	
Total height of rubber (hrt)	5.1 cm (2 in.)		13.3 cm (5.25 in.)		4.8 cm (1.9 in.)	
Ret. anchor bolt dia.	2.5 cm (1.0 in.)		3.8 cm (1.5 in.)		3.2 cm (1.25 in.)	
$P_{RET\_EXPECTED}$	170 kN (38 kips)		377 kN (85 kips)		262 kN (59 kips)	
Fixed bearing	9 × 11		9 × 13		9 × 19	
Plan dims.	23 × 28 cm (9 × 11 in.)		23 × 33 cm (9 × 13 in.)		23 × 48 cm (9 × 19 in.)	
Anchor bolt dia.	1.9 cm (0.75 in.)		3.2 cm (1.25 in.)		2.5 cm (1.0 in.)	
$P_{FIXED\_EXPECTED}$	113 kN (25 kips)		315 kN (71 kips)		200 kN (45 kips)	
Multi-column pier substructure information						
Column clear height	4.5 m (15 ft)	12.2 m (40 ft)	4.5 m (15 ft)	12.2 m (40 ft)	4.5 m (15 ft)	12.2 m (40 ft)
Column diameter	91 cm (36 in.)	91 cm (36 in.)	91 cm (36 in.)	91 cm (36 in.)	91 cm (36 in.)	91 cm (36 in.)
Reinf. ratio (total vert.)	1.07%	1.07%	1.46%	1.46%	1.46%	1.46%
Wall pier substructure information						
Wall clear height	4.5 m (15 ft)	12.2 m (40 ft)	4.5 m (15 ft)	12.2 m (40 ft)	4.5 m (15 ft)	12.2 m (40 ft)
Wall width	10.7 m (35 ft)	10.7 m (35 ft)	10.7 m (35 ft)	10.7 m (35 ft)	10.7 m (35 ft)	10.7 m (35 ft)
Wall thickness	91 cm (36 in.)	91 cm (36 in.)	91 cm (36 in.)	91 cm (36 in.)	91 cm (36 in.)	91 cm (36 in.)
Reinf. ratio (total vert.)	0.28%	0.28%	0.28%	0.37%	0.28%	0.37%

DOI: 10.1002/eqe

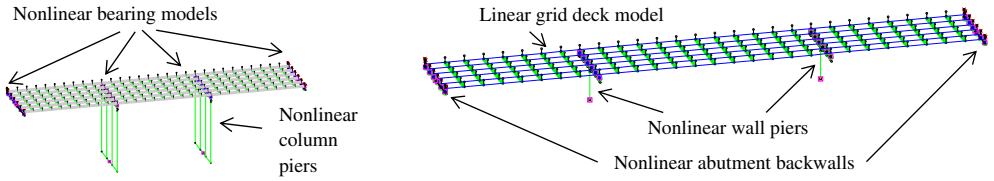

(a) Bridge CsS40T1F (b) Bridge SlW15T1F

Figure 2. Representative finite element meshes for two prototype bridges.

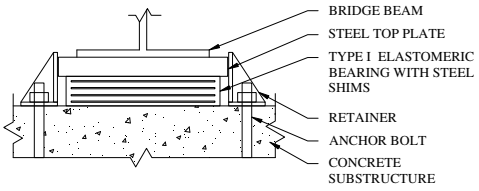

(a) Longitudinal view of Type I elastomeric bearing with steel side retainer

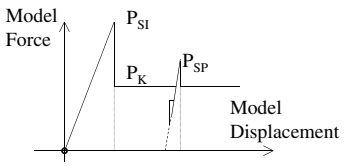

(b) Schematic representation of force-displacement capability of bi-directional model

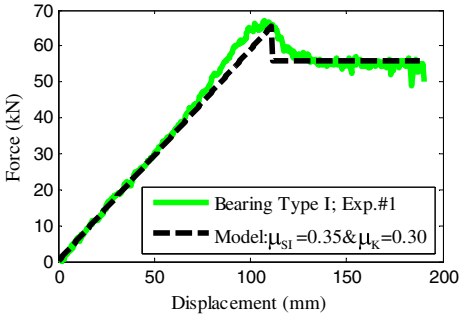

(c) Monotonic experimental behavior of Type I bearing fit with sliding model

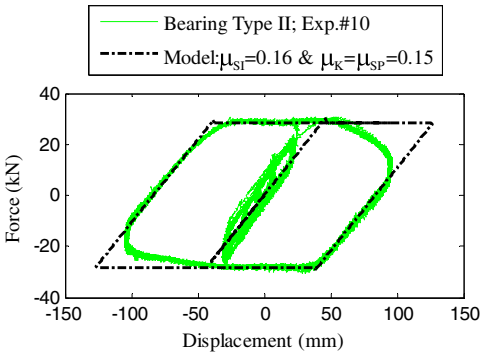

(d) Cyclic experimental behavior of Type II bearing fit with sliding model

Figure 3. Modeling of sliding bearing elements.

on average values from the experimental data. Coupon testing of anchor bolts used in the experiments revealed ultimate material strength of $F_u = 530$ MPa (77 ksi). The model was based on all available data, and pushover analyses showed good correlation with the experimental data, as is shown in Figures 4(a) and (b). For the parametric analyses described in this paper, nominal capacities and material properties were used throughout (e.g., $F_u = 415$ MPa (60 ksi) for anchor bolts).

2.5. Calibration of the bi-directional fixed bearing elements

Low-profile steel bearings, shown in Figure 5, are installed at one of the intermediate substructures to prevent global movements of the bridge deck due to service-level loads. These bearings are normally placed on a 3.2 mm (0.125 in.) elastomeric neoprene leveling pad and are attached to the substructure using anchor bolts. Both the anchor bolts and the steel pintles are designed using the same equations to provide a capacity equal to 20% of the dead load at the bearing; however, because the pintles are typically limited to a minimum diameter of 32 mm (1.25 in.), the anchor bolts are expected to be the critical component that will fail for most bridge configurations.

The nonlinear elasto-plastic deformation of the pintles and anchor bolts, and the friction between the bearing components and substructure, are expected to be an important consideration for the fixed bearing model. A new bi-directional element has been created to simulate the elasto-plastic yielding and fracture of steel components, and can be coupled with the friction element shown in Section 2.3

DOI: 10.1002/eqe

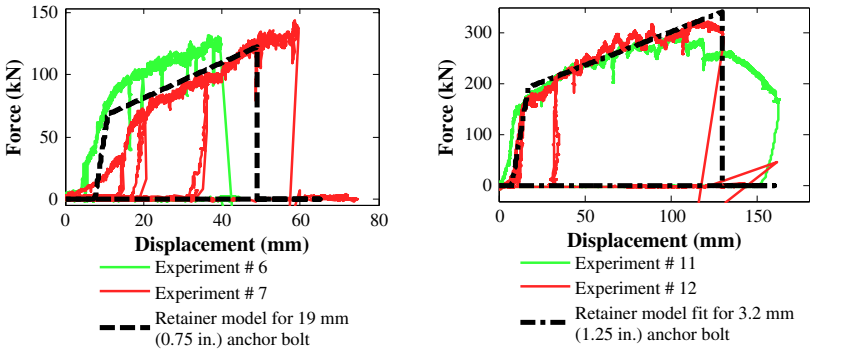

(a) Experimental and model pushover behavior of retainers with 19 mm (0.75 in) anchor bolts

(b) Experimental and model pushover behavior of retainers with 32 mm (1.25 in) anchor bolts

Figure 4. Force–displacement behavior for retainer element experiments and model.

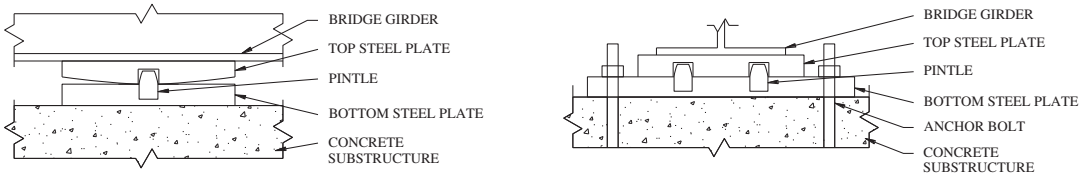

(a) Transverse view

(b) Longitudinal view

Figure 5. Elevation views of low-profile fixed bearings investigated in this research.

of this paper, to capture all important bearing behaviors. A schematic of the model in Figure 6(a) shows a peak-oriented model based on Ibarra *et al*. [16] with variable pinching that follows a predefined elasto-plastic envelope, and is capable of fracturing at a predefined displacement.

The model was verified with the existing experimental data from previous research [17–19] as well as recent testing at the University of Illinois. Figure 6(b) shows the computational model verified against experimental data from the ongoing research, and a further study was performed to

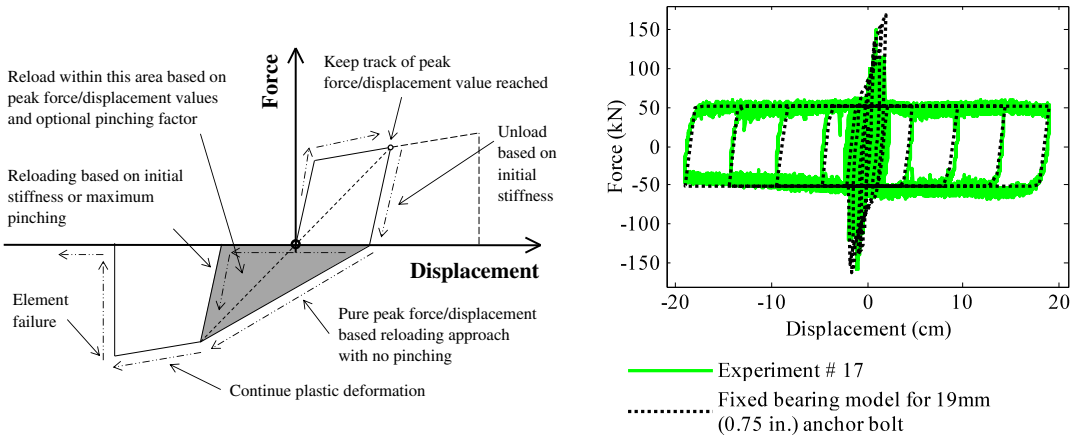

(a) Schematic representation of cyclic behavior of model

(b) Experimental and model cyclic behavior of Low-profile fixed bearings with two 19mm (3/4 in.) anchors

Figure 6. Force–displacement behavior of fixed bearing element model.

DOI: 10.1002/eqe

determine the influence of the fixed bearings on the bridge system [20]. Constant friction ($\mu_{SI} = \mu_{SP} = \mu_K = 0.30$) with the model shown in Section 2.3 was coupled with the fixed bearing model, and the anchor bolt capacity was calculated on the basis of the standard design equation for bolts in shear:

$$P_{\text{FIXED\_EXPECTED}} = \varphi 0.6 * 0.8 A_b F_u \tag{2}$$

This equation uses the factor 0.8 to account for the reduction of anchor bolt area at a threaded section where a nominal diameter (A_b) is used, and the factor of 0.6 is based on the von Mises failure criterion and relates tension and shear strengths, assuming that a pure shear failure occurs in the critical components. The proposed nonlinear model with capacity per Equation (2) with $\varphi = 1$ and $F_u = 415$ MPa (60 ksi) provides a reasonable behavior estimate for the low-profile fixed bearings. A detailed description of the model is available [6], and the formulation can be easily adapted to simulate additional experimental data of other similar fixed bearing components.

3. EARTHQUAKE SIMULATION FOR PARAMETRIC STUDY

The bridges in this parametric study are subjected to response history analyses with different ground motions to assess the impact of several important parameters: the characteristics of the seismic hazard, the intensity of earthquake excitation, and the different directions of shaking.

3.1. Seismic hazard quantification

On the basis of studies of the NMSZ, researchers have developed various synthetic records that model different soil characteristics in the Mississippi embayment [21]. From these ground motions, two sets of 10 synthetic records model a 7% in 75-year exceedence probability (1000-year recurrence event) for southern Illinois for locations with rock (Cape Girardeau, MO–CG records, 10 m soil column) and soil (Paducah, KY–Pa records, 120 m soil column) site conditions. The current research does not include the effects of vertical acceleration because recent research [22] indicates that horizontal-to-vertical component (H/V) spectral ratios for the region are relatively high with values between 2 and 4 in the low-frequency range (frequency ≤ 5 Hz). Furthermore, because the project is aimed at bridges in southern Illinois, a region roughly 200×400 km (125×250 miles) located north of the New Madrid fault zone, and because vertical accelerations attenuate quickly from the source, they are expected to have little effect for most structures in the area. Initial studies of the quasi-isolated systems have also indicated that sliding forces, which may be influenced by vertical accelerations, are typically much smaller and of less significance than the yield capacities of retainers, fixed bearings, and backwalls.

3.2. Scaling of ground motions

The parametric suite contains bridges with elastic first-mode natural periods varying from 0.2 to over 1 s, and effective periods increase greatly as nonlinearities occur during analysis; thus, ground motions were normalized on the basis of a technique used by Somerville *et al*. [23], which uses a least-squares approach to normalize ground motions to a specific target spectrum. The methodology was used to fit the synthetic ground motions to a 1000-year recurrence design spectrum for Cairo, Illinois, from AASHTO [24]. The CG rock records are normalized to the design spectrum for Soil Class B, and the Pa soil records are normalized to the design spectrum for Soil Class D at the location.

Figure 7 shows the ground motion spectra normalized to the respective design spectra, and these ground motions constitute the baseline hazard used in this research. The ground motions as shown are defined to be at a scale factor (SF) of 1.0 and are linearly scaled up and down to provide relative estimates of structural performance for different hazard levels. Cairo, Illinois, has one of the highest hazards for the state and a reasonably high hazard for the NMSZ. Other locations in the region would typically have lower hazards, so as an example the design spectrum hazard in Carbondale, Illinois can be approximated by scaling the baseline ground motions with a factor of 0.5. The

DOI: 10.1002/eqe

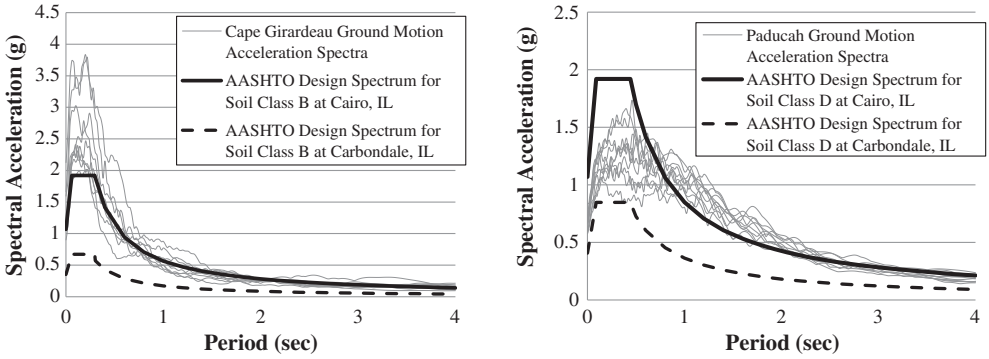

(a) Acceleration spectra for Cape Girardeau normalized to Cairo Soil Class B Hazard (rock)

(b) Acceleration spectra for Paducah normalized to Cairo Soil Class D Hazard (stiff soil)

Figure 7. Spectral acceleration of synthetic ground motion records normalized to the Cairo, Illinois, design spectra.

current research used six distinct SFs (0.5, 0.75, 1.0 = design, 1.25, 1.5, and 1.75) that encompassed different hazard levels to create a coarse IDA [25]. The spectral acceleration of actual earthquake events increases logarithmically for higher magnitude hazards, so the linear scaling used herein does not correspond directly to particular higher hazard levels. However, the maximum considered earthquake (MCE) hazard (2% in 50-year exceedence probability) for the Cairo location can be approximated to be between the 1.5 and 1.75 linearly scaled ground motion levels.

3.3. Directionality effects

Current design provisions [5] recommend that when carrying out calculations in one of the bridge orthogonal directions, in addition to applying the full demand in the direction of interest, 30% of the absolute value of the demand in the perpendicular direction should also be added to account for the directional uncertainty of earthquake motion. Recent research [26] used nonlinear MDOF analyses of symmetric multi-span highway bridges within a stochastic framework to show that the incidence angle is typically negligible in the bridge response. Another work [27], however, has shown that there may be significant variance caused by the incidence angle. Only uni-directional ground motions are available for the region, and the current research focused primarily on the orthogonal application of the ground shaking. Sample studies were carried out with non-orthogonal (45° incident angle) excitation, for the SsC15T2S, SlW15T1F, and CsC40T1S bridge variations, and the findings are discussed in Section 5.2.2.

4. DYNAMIC ANALYSES OF QUASI-ISOLATED SYSTEMS

Dynamic analyses were performed for each bridge configuration with all 20 ground motions scaled independently. Force and displacement data were recorded for each nonlinear component of the bridge at every time step of the ground motion. To allow for concise synthesis of the overall bridge response, individual component responses were aggregated where appropriate. For example, at every substructure, all bearing forces were summed and represented against an average of the bearings' displacements. The bridge SsC15T2S was chosen to show a sample dynamic analysis because this bridge experiences several interesting nonlinearities and also results in a sequence of damage that is discouraged for quasi-isolation.

4.1. Limit states encountered in dynamic analyses of bridges

A list of limit states that can be expected for a typical bridge in both the longitudinal and transverse directions is shown in Table II, and these limit states will hereafter be referred to using the acronyms shown. Limit states can be observed from hysteretic force–displacement response of the various elements, as will be shown in Figures 8 and 11. Unseating of the bearing elements can occur if the bearings slide off of the piers or abutments. This is not explicitly modeled, and therefore, these limit states were determined on the basis of the maximum acceptable displacements. Type I bearings were

DOI: 10.1002/eqe

Table II. Typical limit states observed in bridge prototypes.

Acceptable for quasi-isolation	Acceptable as Level 3 fusing for quasi-isolation
EA—elastomeric bearings slide at abutment	P1—Pier 1 yields
EP—elastomeric bearings slide at Pier 1	P2—Pier 2 yields
RA—retainer failure at abutment	
RP—retainer failure at Pier 1	Discouraged for quasi-isolation
Fb—fixed (low-profile) bearing anchorage failure	UA—unseating of bearing at abutment
Bw—backwall yielding	UP—unseating of bearing at pier

experimentally shown to be reliable when subjected to large slip travel with a gravity-induced average compression stress within the range of 1.38 to 5.52 MPa (200 to 800 psi) [15] , and the model defined in Section 2.3 was considered to be valid as long as there was sufficient contact between the bearing and the concrete substructure. Pier caps and abutment seats were considered to be dimensioned on the basis of the IDOT Bridge Manual [7] equation, which takes into account the width of the superstructure, length between expansion joints, height of the piers, and the 1 s period design spectral acceleration for the bridge. Type I bearing unseating was assumed when any part of the elastomer base extended beyond the edge of the pier cap. Type II bearings were tested to displacements large enough so that the top plate was not in full contact with the bottom plate. Highly nonlinear and unstable behaviors were observed for these bearings when the contact area decreased, so unseating was assumed to occur when the contact distance became less than 7.5 cm (3 in.). For example, Type II 7-b bearings, used at the abutments of steel short (Ss) structures, are assumed to begin unseating at a longitudinal displacement of 10.5 cm (4 in.). Unseating of the bearings can cause extensive damage to the superstructure, substructure, and diaphragm elements, or lead to a local or global collapse of the girders. Also, after unseating occurs, the validity of the computational models becomes questionable and the system is considered to have reached a critical limit state. However, this type of unseating for Type II bearings is not considered unacceptable on the basis of current IDOT ERS philosophy because it does not necessarily lead to a loss of span.

Although a nonlinear model was used to simulate the behavior of the flexible foundation boundary condition, no significant nonlinearity was encountered in the foundation elements, and limit states were not encountered for the foundation systems. Because robust steel H-pile foundations were used both at the abutments and at the piers, other types of foundations used in Illinois may experience more nonlinear behavior under similar seismic excitation. In the future, base shear data from this study can be used to determine if other foundation systems may be applicable for carrying quasi-isolated bridges.

When subjecting a bridge to transverse excitation, the limit states of bearings sliding and retainers failing are technically considered as independent events; however, by inspection of the results, it

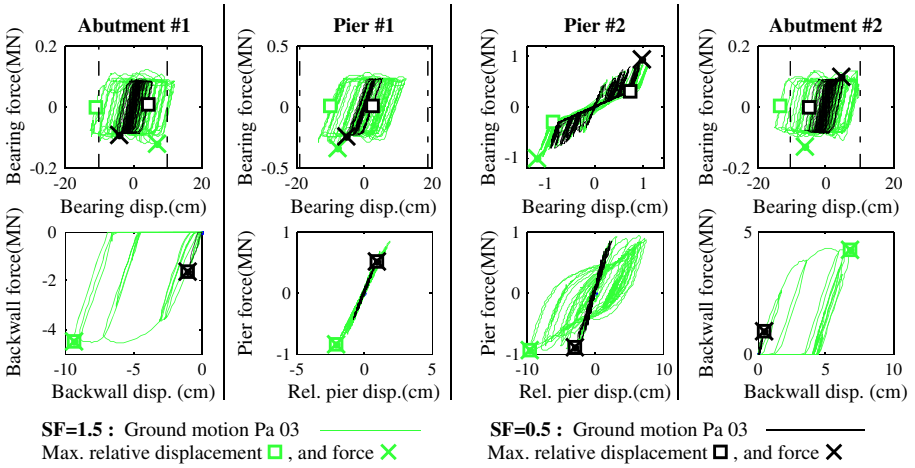

Figure 8. Longitudinal behavior of the SsC15T2S bridge subjected to pure longitudinal excitation.

DOI: 10.1002/eqe

was noted that the retainers had a much larger influence on global behavior than did the bearings. The retainer capacity was the primary factor controlling the force transferred between superstructure and substructure, and until the retainers had failed, the system movement and relative bearing displacements remained essentially zero. Therefore, when considering limit states for transverse analyses, only the retainer failure limit states (RA and RP) are used hereafter, indicating simultaneous occurrence of the elastomeric bearing sliding limit states (EA and EP).

4.2. Longitudinal dynamic behavior of bridge type SsC15T2S

The longitudinal force–displacement hysteretic behaviors of the bearings, backwalls, and piers of the SsC15T2S bridge are shown in Figure 8. The bridge was subjected to pure longitudinal ground shaking from one of the Pa ground motions with SFs of 0.5 and 1.5. The relative pier displacement was calculated by taking the top of the pier displacement and subtracting the foundation shear deformation and the base rotation times the pier height, thereby giving a force–displacement behavior that is comparable for different foundations and pier heights. In Figure 8, the maximum recorded forces and relative displacements are shown with Xs and squares, respectively. Relative displacements of the bearings indicate the magnitude of movement at the sliding interface (i.e., the displacement when the bearing lateral force is unloaded).

Figure 8 shows the occurrence of several interesting nonlinear behaviors for the typical longitudinal analyses. The ground motion applied at SF = 0.5 results in only elastic deformation of the column piers, and there is minor elastic contact with the backwalls. However, when the motion is applied with SF = 1.5, column Pier 2 experiences yielding, the backwall is engaged and experiences nonlinear deformation, and the bearings slide much more, subsequently unseating at Abutment 2 (where the UA limit state is indicated by the vertical dash–dot lines).

Results similar to those presented earlier are available for all components for each individual ground motion analysis. To capture the bridge behavior for the entire suite of ground motions and for varying earthquake intensity, the maximum longitudinal force and displacement quantities are plotted against the earthquake SF, resulting in IDA curves for the bridge response. Figure 9 shows these IDA plots, where a circle is used to show the average response to the suite of 10 Pa ground motions applied at a certain SF, and horizontal bars are used to indicate the range of plus/minus one standard deviation for the data set. The squares and Xs, indicating the maximum displacements and forces specific to the analyses carried out with the Pa 03 ground motion (at SF = 1.5 and 0.5), are also shown on Figure 9. Note that the base shear shown indicates the total force placed on the foundation elements during the analysis.

The IDA curves in Figure 9 also show the incremental behavior for the SsC15T2S bridge, subjected to non-orthogonal shaking at a 45° incident angle. It can be seen that the non-orthogonal analysis

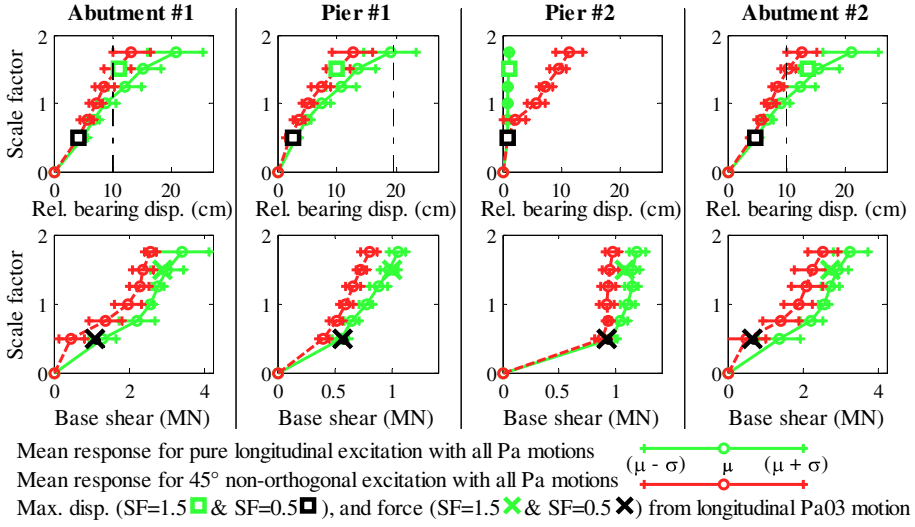

Figure 9. Maximum absolute longitudinal response of the SsC15T2S bridge for incremental hazard.

DOI: 10.1002/eqe

causes the fixed bearing components at Pier 2 to fracture at SF = 1.0 and slide, whereas the pure longitudinal case causes only minor nonlinear behavior. For the non-orthogonal shaking, the coupled longitudinal and transverse forces exceed the bearing capacity, whereas in the pure longitudinal case, Pier 2 experienced yielding before the fixed bearings fracture, as can be observed from the third column of base shear plots shown in Figure 9. Finally, these IDA plots show that, with the exception of the Pier 2 fixed bearing displacements, all other force and displacement responses are greater for the pure longitudinal excitation. The non-orthogonal shaking case also shows similar results when compared with pure transverse excitation in Section 4.3. Similar results were noted from the SlW15T1F and CsC40T1S bridges, and it was concluded that non-orthogonal shaking was overall not as critical as shaking in a single orthogonal direction.

The IDA plots are useful in determining the overall system behavior and the sequence of damage as different limit states occur in different analyses. For instance, in Figure 9, one can see that the base shear at the abutments corresponds to backwall interaction that begins to appear at SF = 0.5, but the forces are lower than those shown in Figure 8 because compacted backfill absorbs a large part of the seismic demand. The base shear for Pier 2 is limited to roughly 1.2 MN (270 kips) as a result of the yielding of the column pier at that substructure. The sequence of damage for the SsC15T2S bridge subjected to Pa ground motions is shown in Figures 10(a) and (c). The bridge experiences yielding of Pier 2 before the design-level earthquake and also bearing unseating at the abutment for SF = 1.25. Both of these limit states are discouraged for a properly quasi-isolated system. A preferred longitudinal sequence of damage for the quasi-isolated system would begin with 'inexpensive' limit states (bearings sliding, EA, and EP) for small earthquakes, followed by relatively easily repaired limit states (Fb and Bw) for design-level earthquakes, and finally would permit damage to substructure elements (P1 and P2) so long as there is no unseating of the bearings. For the IDOT ERS, an underlying preference is that there is no unseating and only modest substructure yielding for SFs of 1.0 or less. Figure 10(b) shows a schematic of a sample acceptable sequence of damage, which is also plotted with square markers in part (c) of that figure. Note that the sequence of damage does not need to follow any particular pattern of damage, as long as limit states do not enter the dark shading indicated in Figure 10(c). As an example, bridge variation SlC40T1F follows an acceptable longitudinal sequence of damage.

4.3. Transverse dynamic behavior of bridge type SsC15T2S

Figure 11 shows hysteretic behavior of the retainers, bearings, and foundations of the SsC15T2S bridge when subjected to pure transverse excitation from one of the Pa ground motions with SFs of 0.5 and 1.5. From the force–displacement plots, it can be seen that the bearings begin to slide primarily after the retainers have failed, and one can also observe some nonlinear behavior in the foundations for the higher earthquake loads. In Figure 12, the maximum absolute values of the transverse response quantities are again transferred onto IDA curves that show the mean and standard deviation for the SsC15T2S bridge considering pure transverse and non-orthogonal

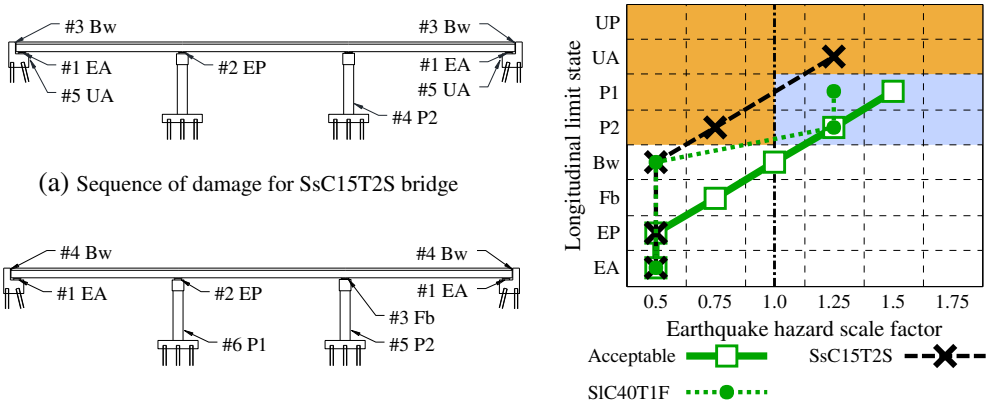

(a) Sequence of damage for SsC15T2S bridge

(b) Sample sequence of acceptable damage

(c) Sequence of damage plot

Figure 10. Sequence of damage representation for incremental longitudinal hazard.

DOI: 10.1002/eqe

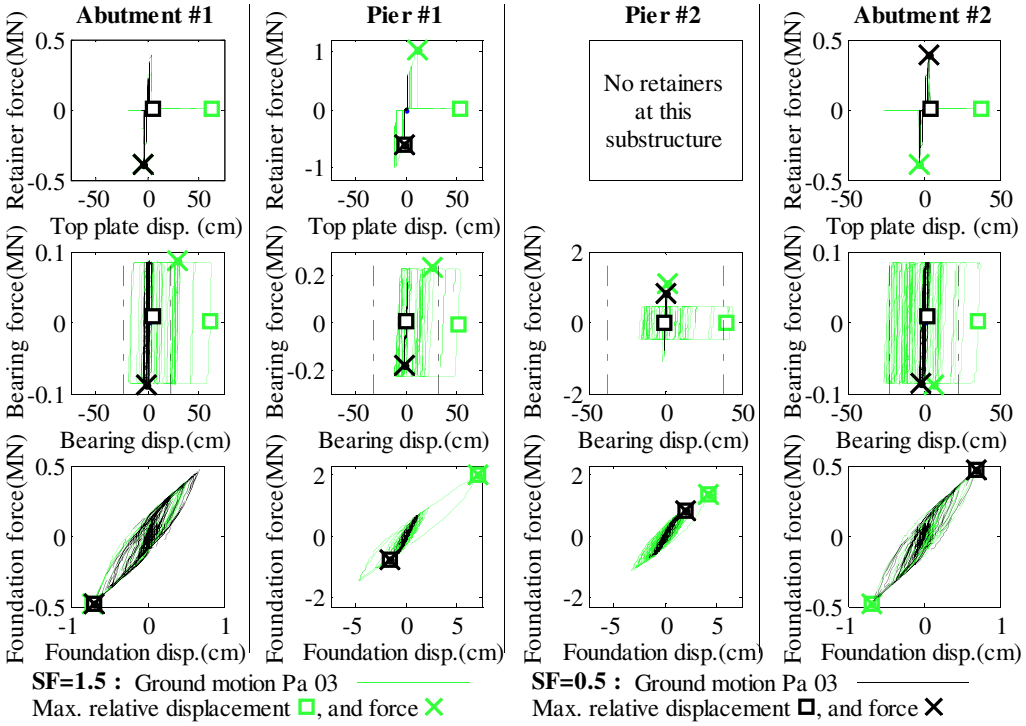

Figure 11. Transverse dynamic behavior of the SsC15T2S bridge subjected to pure transverse excitation.

excitation. The base shears again indicate the total force placed on the foundation components during the analysis. At the abutments, the base shears correspond well to the maximum retainer and bearing sliding forces recorded earlier, whereas the base shears at the piers tend to increase even after bearings and retainers fail. This is because the mass of the piers can cause additional seismic force for higher levels of ground acceleration. The abutment retainers and low-profile fixed bearings fail and permit sliding at a SF of 0.75, and the Pier 1 retainers fuse last at SF = 1.25. After the fuse components have failed, the displacements begin to increase significantly, resulting in abutment and pier bearings unseating at SF = 1.25 and SF = 1.5, respectively. The pure transverse excitation again results in much larger base shears and displacements than the non-orthogonal excitation.

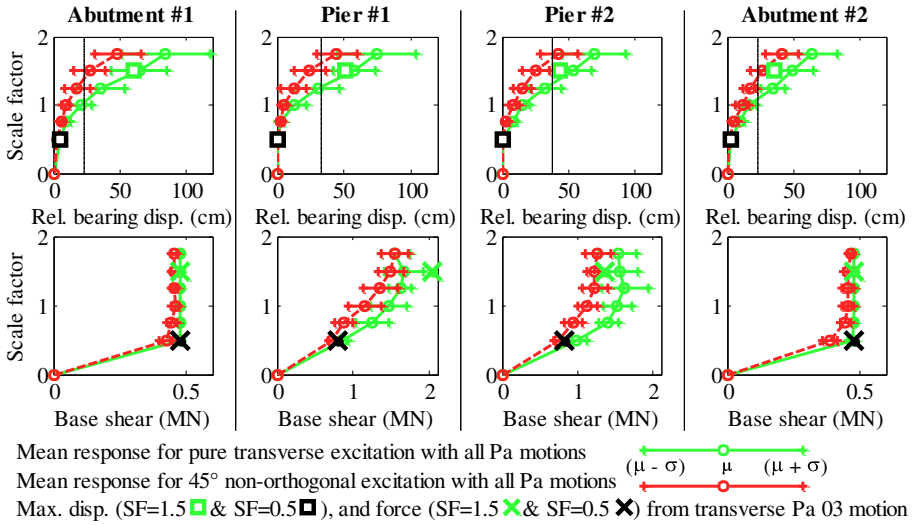

Figure 12. Maximum absolute transverse response of the SsC15T2S bridge for incremental hazard.

DOI: 10.1002/eqe

The transverse sequence of damage for the SsC15T2S structure, as shown in Figure 13, follows an acceptable level of fusing with the exception of the unseating behavior at seismic input levels that are higher than the typical design. An acceptable sequence of damage for the system permits retainer damage (RA and RP) and fixed bearing damage (Fb), as well as column pier yielding (P1 and P2) for larger than design-level earthquakes. An acceptable damage sequence is shown in Figure 13(b) and is plotted with squares in part (c) of the same figure. The CsW40T1F bridge also has an acceptable sequence of damage, as shown in Figure 13(c).

5. RESULTS OF PARAMETRIC STUDY

Results from the entire parametric space, similar to those presented in Section 4, were compared based on the observed sequence of damage, peak displacements, and normalized abutment and pier base shears. The displacements are reported on the basis of the maximum relative displacement of bearings at a single support location, and base shears are normalized with reference to the initial (prior to the seismic analysis) vertical forces at the substructure foundations. Numerical results discussed herein correspond to the performance of the bridge at the design-level earthquake (SF = 1.0), unless otherwise noted.

5.1. Comparison of bridge systems in parametric study

5.1.1. Effect of elastomeric bearings (Type I vs. Type II). Type II bearings typically result in a slight reduction (12%) of Pier 1 base shears, slight reduction (13%) of transverse abutment base shears, and significantly higher displacements (29% longitudinal and 58% transverse). Data for the design-level earthquake (SF = 1) that were used to make these comparisons between bridges with Type I and Type II bearings are shown in Table III. Because of the large amount of data for the various bridge cases, full results are not tabulated here but can be found in [6]. Due to the higher displacement, as well as the different unseating criteria used for Type II bearings, those systems tended to unseat at much lower hazard levels than bridges with Type I bearings. When subjected to the Pa longitudinal excitation, all bridges with tall substructures and Type II bearings (XxX40T2X) (12 out of 24 Type II configurations) unseated at hazard levels at or lower than the design-level earthquake (SF = 1.0), and almost all bridges with Type II bearings had unseated for SF = 1.75 for both the CG and Pa ground motions. In the transverse direction, similar behavior was observed for the bridges with Type II bearings, with 15 out of 24 Type II cases unseating before SF = 1 for the Pa motions, and all 24 bridges unseating by SF = 1.75 for both Pa and CG motions.

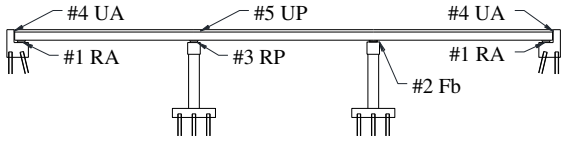

(a) Sequence of damage for SsC15T2S bridge

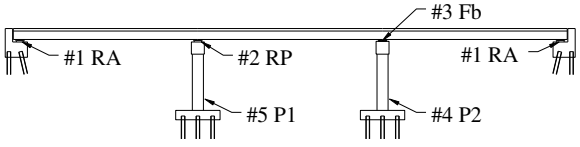

(b) A sample sequence of acceptable damage

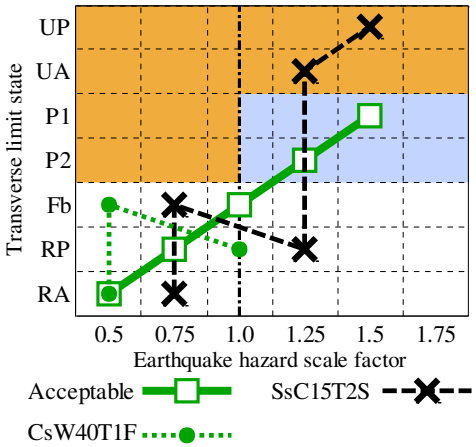

(c) Sequence of damage plot

Figure 13. Sequence of damage representation for incremental transverse hazard.

DOI: 10.1002/eqe

Table III. Displacement and force response comparison between bridges with Type I and Type II bearings at a design-level earthquake (SF = 1).

	Average max. relative bearing displacement (cm)			Average maximum normalized pier base shears (no units)						Average maximum normalized abutment base shears (no units)					
				T1		T2		(T2 − T1)/T1		T1		T2		(T2 − T1)/T1	
Ground motion suite	T1	T2	(T2 − T1)/T1	Pier 1	Pier 2	Pier 1	Pier 2	Pier 1	Pier 2	Abut 1	Abut 2	Abut 1	Abut 2	Abut 1	Abut 2
Longitudinal															
Pa	12.6	16.2	0.29	0.31	0.34	0.27	0.34	−0.13	−0.02	3.69	3.66	3.59	3.50	−0.03	−0.04
CG	7.0	8.9	0.28	0.34	0.34	0.31	0.33	−0.07	−0.03	3.21	3.22	2.98	2.97	−0.07	−0.08
Mean	9.8	12.6	0.29	0.32	0.34	0.29	0.33	−0.10	−0.03	3.45	3.44	3.29	3.24	−0.05	−0.06
Transverse															
Pa	18.9	28.8	0.53	0.63	0.58	0.54	0.58	−0.15	0.00	0.95	0.96	0.83	0.83	−0.13	−0.14
CG	8.1	13.9	0.72	0.51	0.51	0.45	0.51	−0.13	−0.01	0.94	0.94	0.83	0.82	−0.12	−0.12
Mean	13.5	21.4	0.58	0.57	0.55	0.49	0.54	−0.14	−0.01	0.94	0.95	0.83	0.82	−0.13	−0.13

DOI: 10.1002/eqe

Type I bearing systems on the other hand performed much better, with no unseating recorded for longitudinal excitation. For transverse excitation with Pa ground motions, seven out of 24 bridges unseated at SF = 1.5, and an additional eight bridge variants unseated at SF = 1.75. Of these cases, bridges with flexible foundation boundary conditions typically unseated at lower SFs. No transverse unseating was recorded for Type I bearing systems for the CG ground motions, so these bridges are only considered vulnerable for high seismic hazards. Figure 14 shows comparisons of bridge systems, and it indicates that bridges with Type II bearings are more susceptible to unseating damage than similar bridges with Type I bearings. Type II bearings have a lower coefficient of friction and therefore provide less resistance to sliding, and they also have a more restrictive unseating definition, as noted earlier on the basis of experimental results. Unseating should be avoided because it can cause damage in superstructure and diaphragm elements and can potentially lead to local or global collapse.

5.1.2. Effect of substructure type (multi-column pier vs. wall pier) and substructure height (4.5 m (15 ft) vs. 12.2 m (40 ft)). For longitudinal analyses, most wall and multi-column pier bridges followed a sequence of damage where Pier 2 was damaged at low earthquake SFs (0.5 or 0.75). Most tall structure variants (XxX40) and short pier structures with Type I bearings of Sl and Cs variants (SlX15T1 and CsX15T1) experienced yielding in both the isolated and non-isolated piers, Piers 1 and 2, respectively, before the design-level earthquake. For the remaining short substructure bridge variants, Pier 1 was isolated and protected from damage up to the design-level earthquake, but above the design level, Pier 1 yielded in all except XxC15T2 variants.

For transverse excitation, short multi-column pier substructures (XxC15) and all wall substructures (XxW##) were typically strong enough that the fixed bearings and Pier 1 retainers failed, thereby allowing for effective quasi-isolation. One exception was the steel long bridges (Sl) where some pier yielding was noted to occur before the design-level earthquake for the short column pier variants. When subjected to transverse excitation, most tall multi-column pier substructures (XxC40) yielded before reaching the design-level earthquake, and the Pier 1 retainers and low-profile fixed bearings remained essentially elastic even at high levels of seismic excitation.

Bridges with tall pier substructures, on average, experienced maximum deformations that were 74% and 24% larger than their short pier equivalents for longitudinal and transverse excitations, respectively. These higher displacements often resulted in unseating failures, as was noted in Section 5.1.1. The tall pier substructures experienced lower normalized base shears than short pier bridges by 39% for longitudinal and 30% for transverse excitation. The difference in base shears can be attributed to the fact that the base shears were capped by the lateral yield capacity of the substructures, which were lower for the taller piers. Backwall forces, however, increased by 12% for the taller bridge variations. In comparison with column pier bridges, the normalized base shears at wall piers were 20% higher in the longitudinal and 18% higher in the transverse directions, which

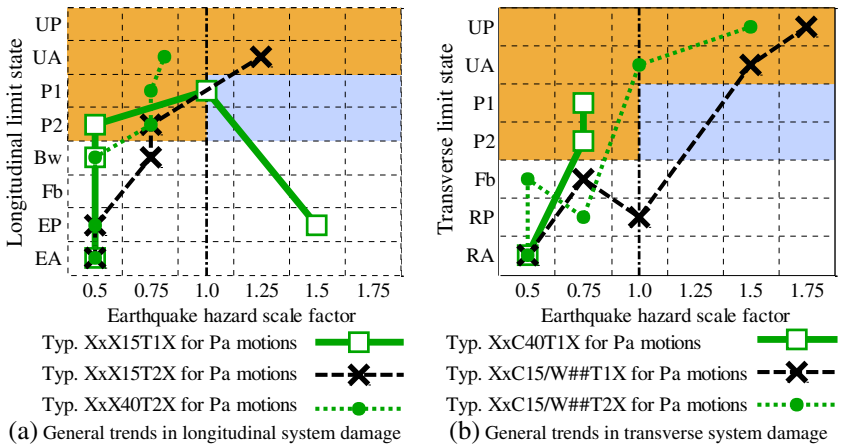

Figure 14. General trends of system damage for some typical bridge cases.

DOI: 10.1002/eqe

can again be attributed to the yield capacity of the different systems. The abutment force and displacement response did not vary significantly between column and wall pier systems, and the longitudinal pier response was also similar for the two systems. In the transverse direction, however, wall piers are much stiffer than column piers and experienced 177% higher pier bearing displacements and roughly 20% higher normalized pier base shears.

5.1.3. Effect of superstructure type (steel short/steel long/concrete short). As is discussed in Section 5.1.2, the steel long (Sl) superstructures often experienced pier yielding earlier than the other superstructures. This can be attributed to the higher axial load at the substructures, as well as the higher fuse capacities, which are designed as a factor of the dead load. System displacements increased with superstructure length, and the steel short (Ss) superstructure generally had slightly higher normalized base shears. This is primarily because the substructure mass was higher when compared with the superstructure. There were slight differences in displacement between the three cases, as the bridges differ in structural period. However, the systems performed about equivalently in terms of unseating, so the seat width equations effectively incorporate superstructure length.

5.1.4. Effect of foundation stiffness (fixed vs. flexible boundary condition). Bridge cases with flexible foundation conditions experienced generally small differences in bearing displacement and normalized base shear when compared with the fixed foundation variations. Because the flexible foundations could accommodate some displacement, their presence at times altered the sequence of damage such that piers and fixed bearings experienced lower forces and were thereby damaged at higher SFs of excitation, or were not damaged at all. Because of the higher displacement demands, flexible variations were somewhat more prone to unseating, typically reaching the UA or UP limit state at a SF of about 0.25 lower that what was observed for fixed foundation cases (i.e., unseating at SF = 1.5 vs. SF = 1.75).

5.2. Other observations on bridge performance

5.2.1. Effect of ground motion type (CG motions vs. Pa motions). Results for all 48 bridge variants subjected to Pa ground motions were compared with results from the CG ground motions at the design-level earthquake hazard. Under longitudinal excitation, Pa ground motions resulted in 81% higher bearing displacements, 4% lower intermediate substructure base shears, and 20% higher abutment backwall forces than the CG counterparts. For transverse excitation, the Pa motions resulted in 116% higher bearing displacements and 18% higher base shears at the intermediate substructures, and the abutment base shears remained equivalent because they were limited by the retainer and bearing sliding force capacity for both types of excitation. The increase in base shear and displacements was more significant in structures with longer periods (i.e., Sl vs. Ss superstructure, tall vs. short substructure, and flexible vs. fixed base) that were more susceptible to lower frequency excitation. By general observation of damage patterns in the entire parametric space, it was noted that the Pa and CG motions produce approximately the same sequence of damage, but the Pa motions normally result in limit states being reached at lower SFs of excitation than with the CG motions. For example, in the transverse direction, 31% more bridges experienced unseating when subjected to the Pa than the CG motions.

5.2.2. Non-orthogonal (45° incident angle) application of ground motions. Non-orthogonal seismic excitation was found to be equal or less critical compared with uni-directional ground motion application for the quasi-isolated system studied in this paper. The SsC15T2S, SlW15T1F, and CsC40T1S bridge variations were studied with uni-directional and non-orthogonal excitation, and it was determined that the mean bridge response was less for non-orthogonal ground motion application. As can be observed from Figures 9 and 12, the non-orthogonal excitation can often alter the sequence of damage (that is, cause bearing failure or pier yielding) before it would occur in one of the orthogonal directions, but the peak displacements and base shears would still be recorded for cases where pure orthogonal excitation is applied. This behavior occurs because the bridge tested with non-orthogonal excitation takes advantage of multiple lateral systems, including the side retainers and strong axis of the pier substructures for the transverse force component, and the abutment backwall for the longitudinal force component.

DOI: 10.1002/eqe

5.2.3. Performance of bridge systems within the New Madrid Seismic Zone. It is important to note that the ground motions used in this study were initially normalized to design spectra for Cairo, Illinois, which is nearly the highest hazard for Illinois and the NMSZ in general. This level of hazard was chosen as the baseline for this study to establish an upper bound on response for Illinois bridges. Bridges with quasi-isolation systems farther away from the NMSZ and with lower hazard levels are expected to experience significantly less damage than those shown in this study. The parametric variations used in this study provide a representative sample of modern bridges in Illinois that employ elastomeric bearings and simply supported abutment conditions. The chosen pier heights, span lengths, foundation stiffnesses, and ground motions provide a reasonable selection of common bridge cases in the NMSZ, and it is reasonable to apply the results and recommendations presented herein to similar structures.

The results from this research are generally consistent with other studies on bridges in the NMSZ. When studying fragilities of wall pier bridges in Illinois, Bignell and LaFave [28] found that overall, bridge systems in the region are expected to experience only moderate damage for the MCE-level hazard, which is similar to the conclusions herein. Similarly, they noted that pier properties were important in the general bridge response, but in contrast to the study presented in this paper, they found that bearings (steel roller, low-profile fixed, and elastomeric in some cases) had little influence on the bridge fragility. A study of multi-span simply supported bridges by Nielson and DesRoches [29] showed that for the MCE-level hazard, significant vulnerabilities exist at the piers, at the abutments, and in the unseating of girders. The study found that longitudinal and transverse displacement demands were of the same order, whereas the IDA results shown herein indicate that for continuous bridges, transverse deformations tend to be much greater than longitudinal, especially at higher degrees of excitation. The difference in deformation demand can be attributed to the bearings used in the previous research, where steel dowels at the intermediate substructures did not fuse and permit sliding as is intended for quasi-isolated systems.

6. CONCLUSIONS

This research investigated the seismic performance of typical bridge configurations currently used in the state of Illinois. The analyzed bridges featured different superstructures, substructures, foundation stiffnesses, and types of elastomeric bearings. The structures were selected as a representative sample of bridges in southern Illinois, and performance observations can be generalized to similar systems in the region. Bridge response was studied using nonlinear numerical models where transient seismic analyses were carried out for incremental hazard levels. The parametric analyses point to the following conclusions:

- From the current parametric study, only a few bridge variants were noted to unseat for design-level earthquakes, indicating that most structures in Illinois would not experience severe damage during their typical design life. Because a high hazard level was used as a baseline to scale the ground motions, unseating and span loss are not likely for regions with moderate seismic hazard.
- Bridges with Type II IDOT bearings were shown to be more prone to unseating, as the area of the bearing surface often proved to be insufficient given the magnitude of the displacement demand. Unseating of the bearings is an unstable and unpredictable behavior leading to large displacements, potential damage to deck and diaphragm elements, and possible local or global collapse. Tall structures with Type II bearings experienced longitudinal unseating before design-level earthquakes, and nearly all bridges with Type II bearings experienced both transverse and longitudinal unseating for MCE-level hazards.
- Bridges with Type I bearings showed reliable behavior in preventing system collapse. No unseating was noted for longitudinal excitation of these bridges, and unseating of the bearings in the transverse direction was only observed at MCE-level hazard for ground motions scaled on the basis of a design spectrum for Soil Class D ground motions.
- The sequence of damage of most bridge structures indicates some yielding of the piers with fixed bearings for small earthquakes and potential unseating of some bridges for large seismic events,

DOI: 10.1002/eqe

which are both discouraged for quasi-isolation. Calibration of fuse component capacities and revision of seat width equations can improve the sequence of damage for many bridge systems.

- Displacements in the longitudinal direction are generally much lower than in the transverse direction because of the influence of the backwall elements. For design-level earthquakes, transverse bearing displacements were roughly 36% higher than the longitudinal, and the transverse displacements increased faster as the intensity of the earthquake increased. This difference arises because after the retainers and fixed bearings have failed, there is no active restraint of the system in the transverse direction.
- Bridge displacement response was noted to be significantly larger for systems with tall pier substructures and Type II bearings.
- Ground motions simulating soil site conditions and scaled on the basis of a design spectrum for Soil Class D typically resulted in larger force and displacement demands than rock ground motions, which were scaled on the basis of a design spectrum for Soil Class B, of similar intensity. The soil ground motions also resulted in more limit states being reached at lower hazard levels.

ACKNOWLEDGEMENTS

This paper is based on the results of ICT R27-70, *Calibration and Refinement of Illinois' Earthquake Resisting System Bridge Design Methodology*. ICT R27-70 was conducted in cooperation with the Illinois Center for Transportation (ICT); IDOT, Division of Highways; and the US Department of Transportation, Federal Highway Administration (FHWA). The contents of this paper reflect the view of the authors, who are responsible for the facts and the accuracy of the data presented herein. The contents do not necessarily reflect the official views or policies of the ICT, IDOT, or FHWA. The authors would like to thank the members of the project Technical Review Panel, chaired by D. H. Tobias, for their valuable assistance with this research. Grid resources from the Texas Advanced Computing Center (TACC) at The University of Texas at Austin were used to generate research results reported within this paper.

REFERENCES

1. Buckle IG. Seismic isolation: history, application, and performance—a world view. *Earthquake Spectra* 1990; **6**(2): 161–201.
2. Tobias DH, Anderson RE, Hodel CE, Kramer WM, Wahab RM, Chaput RJ. Overview of earthquake resisting system design and retrofit strategy for bridges in Illinois. *Practice Periodical on Structural Design and Construction* 2008; **13**(3):147–158.
3. Buckle IG, Constantinou MC, Dicleli M, Ghasemi H. Seismic Isolation of Highway Bridges, MCEER Report 06-SP07, University of Buffalo. 2006.
4. American Association of State Highway and Transportation Officials(AASHTO). *Guide Specifications for Seismic Isolation Design*—Third Edition. American Association of State Highway and Transportation Officials (AASHTO): Washington, D.C. 2010.
5. AASHTO. Guide specifications for LRFD seismic bridge design with interims. American Association of State Highway and Transportation Officials (AASHTO): Washington, D.C. 2009.
6. Filipov ET. Nonlinear seismic analysis of quasi-isolation systems for earthquake protection of bridges. Thesis, University of Illinois at Urbana Champaign, Urbana, Illinois, 2012.
7. Illinois Department of Transportation (IDOT), Bridge Manual. Springfield, IL, 2009.
8. Filipov ET, Fahnestock LA, Steelman JS, Hajjar JF, LaFave JM, Foutch DA. Evaluation of quasi-isolated seismic bridge behavior using nonlinear bearing models. *Engineering Structures*. Accepted 2012. doi:10.1016/j.engstruct.2012.10.011
9. Bignell JL, LaFave JM, Hawkins NM. Seismic vulnerability assessment of wall pier supported highway bridges using nonlinear pushover analyses, *Engineering Structures* 2005; **27**(14):2044–2063.
10. McKenna F, Mazzoni S, Fenves GL. Open System for Earthquake Engineering Simulation (OpenSees). University of California, Berkeley, CA. http://opensees.berkeley.edu/, 2006. (23 September 2011)
11. Becker TC, Mahin SA. Experimental and analytical study of the bi-directional behavior of the triple friction pendulum isolator. *Earthquake Engineering and Structural Dynamics* 2011. DOI: 10.1002/eqe.1133
12. Mosqueda G, Whittaker AS, Fenves GL. Characterization and modeling of friction pendulum bearings subjected to multiple components of excitation. *Journal of Structural Engineering* 2004; **130**(3):433–442.
13. Constantinou MC, Mokha A, Reinhorn A. Teflon bearings in base isolation II: modeling. *Journal of Structural Engineering* 1990; **116**(2):455–474.
14. Steelman JS, Fahnestock LA, LaFave JM, Hajjar JF, Filipov ET, Foutch DA. Seismic response of bearings for quasi-isolated bridges—testing and component modeling. Structures Congress, Las Vegas, NV, 2011.
15. Steelman JS, Fahnestock LA, Filipov ET, LaFave JM, Hajjar JF, Foutch DA. Shear and friction response of non-seismic laminated elastomeric bridge bearings subject to seismic demands. *Journal of Bridge Engineering* 2012; (April 26): DOI:10.1061/(ASCE)BE.1943-5592.0000406.

16. Ibarra IF, Medina RA, Krawinkler H. Hysteretic models that incorporate strength and stiffness deterioration. *Earthquake Engineering and Structural Dynamics* 2005; **34**(12):1489–1511.
17. Mander JB, Kim DK, Chen SS, Premus GJ. Response of steel bridge bearings to reversed cyclic loading. Report NCEER-96-0014 State University of New York at Buffalo, Buffalo, NY, 1996.
18. Klinger RE, Mendoca JA, Malik JB. Effect of reinforcing details on the shear resistance of anchor bolts under reversed cyclic loading. *ACI Journal* 1982; **79**(1):3–12.
19. Gomez I, Kavinde A, Smith C, Deierlein G. Shear transfer in exposed column base plates. AISC report, University of California, Davis & Stanford University 2009.
20. Filipov ET, Revell JR, Steelman JS, Fahnestock LA, LaFave JM, Foutch DA, Hajjar JF. Sensitivity of quasi-isolated bridge seismic response to variations in bearing and backwall elements. Paper No. 2978, Proceedings of the 15th World Conference on Earthquake Engineering, Lisbon, Portugal, 2012.
21. Fernandez JA, Rix GJ. Seismic hazard analysis and probabilistic ground motions in the upper Mississippi embayment. 2008. ASCE Conference Proceedings. DOI:10.1061/40975(318)8.
22. Zandieh A, Pezeshk S. A Study of horizontal-to-vertical component spectral ratio in the New Madrid Seismic Zone. *Bulletin of the Seismological Society of America* 2011; **101**(1):287–296.
23. Somerville P, Smith N, Punyamurthula S, Sun J. Development of ground motion time histories for phase 2 of the FEMA/SAC steel project. SAC/BD-97/04, Sacramento, CA, 1997.
24. AASHTO. Seismic Design Paramaters CD. American Association of State Highway and Transportation Officials (AASHTO), 2008.
25. Vamvatsikos D, Cornell CA. Incremental dynamic analysis. *Earthquake Engineering and Structural Dynamics* 2002; **31**(3):491–514.
26. Mackie KR, Cronin KJ, Nielson BG. Response sensitivity of highway bridges to randomly oriented multi-component earthquake excitation. *Journal of Earthquake Engineering* 2011; **15**(6): 850–876. DOI: 10.1080/13632469.2010.551706
27. Bisadi V, Head M. Orthogonal effects in nonlinear analysis of bridges subjected to multicomponent earthquake excitation, Structures Congress 2010. DOI:10.1061/41130(369)20
28. Bignell J, LaFave J. Analytical fragility analysis of southern Illinois wall pier supported highway bridges. *Earthquake Engineering and Structural Dynamics* 2010; **39**(7):709–729.
29. Nielson BG, DesRoches R. Seismic performance assessment of simply supported and continuous multispan concrete girder highway bridges. *Journal of Bridge Engineering* 2007; **12**(5):611. DOI:10.1061/(ASCE)1084-0702 (2007)12:5(611)